Ceramic fibres from polymer precursor containing Si–O–Ti bonds

Part II *Synthesis of various types of ceramic fibres*

YOSHIO HASEGAWA
The Research Institute for Special Inorganic Materials, Asahi-mura, Kashima-gun, Ibaraki-ken 311-14, Japan

CHUN-XIANG FENG, YONG-CAI SONG, ZI-LIE TAN
The Department of Materials Science and Applied Chemistry, Changsha Institute of Technology, Changsha, Hunan, People's Republic of China

Polycarbosilanes containing titanium alkoxide as pendant groups (atom ratio Ti/Si = 0.07 and 0.15) were synthesized. These polymers were melt-spun and then heat-treated in a vacuum, in oxygen or ammonia gas flow, resulting in Si–Ti–C–O, Si–Ti–O and Si–Ti–O–N fibres, respectively. The pyrolysis process of the polymer is discussed in connection with the mechanical properties and the structure of the fibre. At high heat-treatment temperatures, β-SiC and TiC (in Si–Ti–C–O fibre), anatase (in Si–Ti–O fibre) and TiN (in Si–Ti–O–N fibre) crystallized, which may be closely related to the decomposition of the Si–O–Ti bond in the fibre.
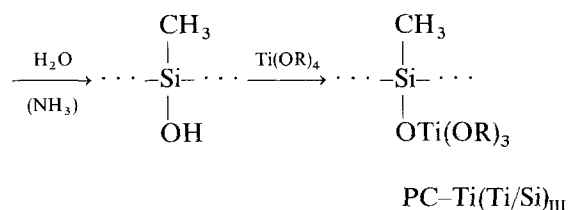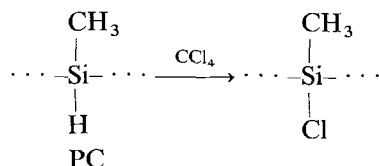
1. Introduction

The method of synthesis of organosilicon polymer containing Si–O–Ti bonds using some reactions between organosilicon compounds, such as polycarbosilane (PC), and titanium alkoxide were reported previously; the polymers obtained are useful as precursors for ceramics [1]. The introduction of other metallic elements into the PC is not only regarded as a means of improving the mechanical properties of ceramics obtained from PC, for example SiC fibre, but is also important in producing high-performance ceramics with polymer precursors. Pyrolysis of the precursor under different atmospheres also gives various ceramics with different compositions such as carbide, oxide, nitride, etc.

In the present study, using PC containing titanium alkoxide as a pendant group synthesized by the method reported previously [1], the pyrolysis process of the precursor and the structure of the pyrolysis product were examined. The mechanical properties of Si–Ti–C–O, Si–Ti–O and Si–Ti–O–N fibres obtained from this precursor were also studied.

2. Experimental procedure

2.1. Synthesis of polymers

The precursor polymers were synthesized by method III [1] in which a titanium alkoxide is introduced to the silicon atom bonded with a hydrogen atom as a pendant group as follows

$$\cdots \underset{\underset{\text{PC}}{\overset{|}{\underset{H}{}}}}{\overset{\overset{CH_3}{|}}{-Si-}} \cdots \xrightarrow{CCl_4} \cdots \underset{\overset{|}{Cl}}{\overset{\overset{CH_3}{|}}{-Si-}} \cdots$$

$$\xrightarrow[(NH_3)]{H_2O} \cdots \underset{\overset{|}{OH}}{\overset{\overset{CH_3}{|}}{-Si-}} \cdots \xrightarrow{Ti(OR)_4} \cdots \underset{\overset{|}{OTi(OR)_3}}{\overset{\overset{CH_3}{|}}{-Si-}} \cdots$$

$$PC–Ti(Ti/Si)_{III}$$

The polymer obtained is termed $PC–Ti(Ti/Si)_{III}$ from the atomic ratio Ti/Si when PC and titanium alkoxide were mixed. For titanium alkoxides, tetraisopropoxititanium (TPT) or tetrabutoxititanium (TBT) was used.

In this study, $PC–Ti(0.07)_{III}$ obtained from PC–B1.0–350 ($SiC_4 = 0.23$, $SiC_3H = 0.23$ and $SiC_xSi_{4-x} = 0.54$, number-average molecular weight, $\bar{M}_n = 920$) [2] and TPT, and $PC–Ti(0.15)_{III}$ obtained from PC–350 ($SiC_4 = 0.27$, $SiC_3H = 0.24$ and $SiC_xSi_{4-x} = 0.49$, $\bar{M}_n = 560$) [2] and TBT were used.

2.2. Synthesis of ceramic fibres

$PC–Ti(Ti/Si)_{III}$ was melted at 150 to 160 °C under a nitrogen atmosphere, and melt-spun into fibre which was then cured by leaving in atmospheric air at room temperature (RT) for 1 day or more, or heating in air at a specified temperature (T_c, the curing temperature) for 1 h at a heating rate of $10\,°C\,h^{-1}$ from room temperature. Subsequently, the cured fibre was heat treated in a vacuum of about 3×10^{-3} torr or in an oxygen or ammonia gas flow of $200\,cm^3\,min^{-1}$ up to a specified temperature and held for 1 h at that temperature. The heating rate was $100\,°C\,h^{-1}$ in a vacuum and an oxygen gas flow, and $200\,°C\,h^{-1}$ in ammonia gas flow. The heat treatment of the cured fibre was performed in a tubular furnace (50 mm diameter).

Thus, the various types of ceramic fibres, i.e. Si–Ti–C–O, Si–Ti–O and Si–Ti–O–N fibres were synthesized. The average diameters of the fibres obtained from $PC–Ti(0.07)_{III}$ and $PC–Ti(0.15)_{III}$ were 11 to 12 μm and 13 to 17 μm, respectively.

2.3. Measurements
Infrared spectra, the molecular weight distribution and $\bar{M}_n$ were measured in the same manner as reported previously [1]. The tensile strength and Young's modulus of the fibre were measured at room temperature with a universal testing machine UTM-II-20 (Toyo Baldwin Co., Tokyo, Japan) with a 25 mm gauge length and a cross-head speed of 2 mm min^{-1}. Thirty specimens of the fibres were measured, and the average value and standard deviation were determined. The X-ray diffraction pattern (CuK_α) of the fibre was measured with a Miniflex (Rigaku Co., Tokyo, Japan). The carbon content in the fibre was measured with a carbon analyser model EMIA-110 (Horiba Ltd, Kyoto, Japan). Observation of the fibre was made by scanning electron microscopy (SEM) JSM-840 (Jeol Ltd, Tokyo, Japan).

3. Results and discussion
3.1. Characterization of the polymers
The structures and properties of the polymer precursors have been reported previously [1]. Fig. 1 shows the molecular weight distributions of $PC–Ti(0.07)_{III}$ and $PC–Ti(0.15)_{III}$. In $PC–Ti(0.07)_{III}$, it was found that TPT is introduced into the PC molecule as a pendant group, $-OTi(OC_3H_7)_3$, because the molecular weight distribution is almost the same as that of the starting PC–B1.0–350. On the other hand, the molecular weight distribution of $PC–Ti(0.15)_{III}$ shows the formation of higher molecular weight components than PC–350 and, consequently, the introduction of TBT as a bifunctional or trifunctional agent intermolecularly cross-linking PC. This is the reason why the spinnability of $PC–Ti(0.15)_{III}$ is lower than that of $PC–Ti(0.07)_{III}$ and, consequently, the fibre diameter of $PC–Ti(0.15)_{III}$ is larger than that of $PC–Ti(0.07)_{III}$.

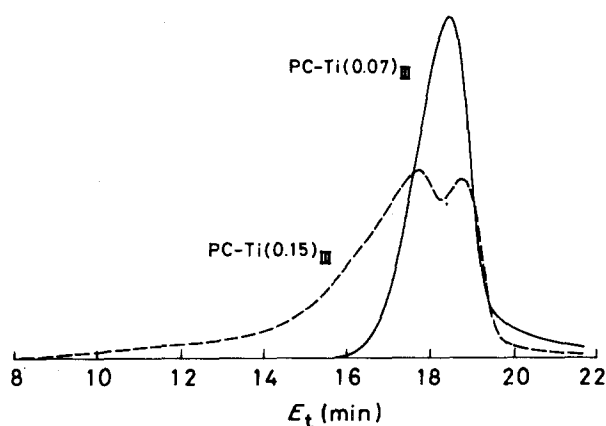Characterization of the pyrolysis process of the polymer will be described later.

3.2. Si–Ti–C–O fibre
In the pyrolysis process of the polymer in an inert gas atmosphere and in a vacuum, it has been shown that the Si–O–Ti bond is cleaved by pyrolysis of the Ti–O bond, so that TiC is formed [1]. In Fig. 2, the change in the infrared spectrum of $PC–Ti(0.07)_{III}$ pyrolysed in a nitrogen gas flow of 100 cm^3 min^{-1} is shown. For infrared spectrum measurements, the KBr disc was heat-treated repeatedly at 200 to 700 °C for 1 h. The absorption peak at 890 cm^{-1} due to the Si–O–Ti bond decreases with increasing temperature, and almost disappears at 400 °C. The absorption peak at 600 to 700 cm^{-1} due to the Ti–O bond also decreases. The peak intensity at 1000 to 1100 cm^{-1}, on the other hand, increases with increasing temperature. Therefore, Fig. 2 shows that the Si–O–Ti and Ti–OR bonds in $PC–Ti(0.07)_{III}$ are decomposed and the Si–O–Si bond is formed.

As can be seen from Fig. 2, the pyrolysis of PC forming the skeleton of the polymer is predominant above 400 °C. The formation of the Si–H (2100 cm^{-1}) and Si–CH$_2$–Si (1355 cm^{-1}) bonds is also observed, due to the decomposition of SiC_xSi_{4-x} in PC–B1.0–350. These changes are the same as those of PC during pyrolysis [3].

$PC–Ti(0.07)_{III}$ and $PC–Ti(0.15)_{III}$ were melt-spun and then cured. Both cured fibres, namely $PC–Ti(0.07)_{III}$ fibre $(T_c = RT$ or 110 °C) and $PC–Ti(0.15)_{III}$ fibre $(T_c = RT)$, were heat-treated in a vacuum. The relation between the mechanical properties of the resulting fibre (Si–Ti–C–O fibre) and heat-treatment temperature are shown in Fig. 3. Both the tensile strength and Young's modulus decrease above
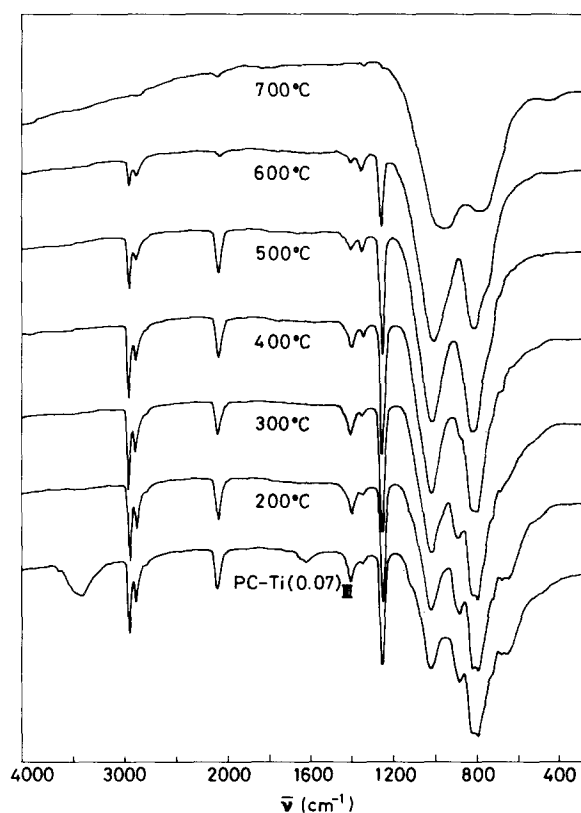

Figure 1 GPC curves of $PC–Ti(0.07)_{III}$ and $PC–Ti(0.15)_{III}$.

Figure 2 Change in infrared spectrum of $PC–Ti(0.07)_{III}$ pyrolysed in the KBr disc.

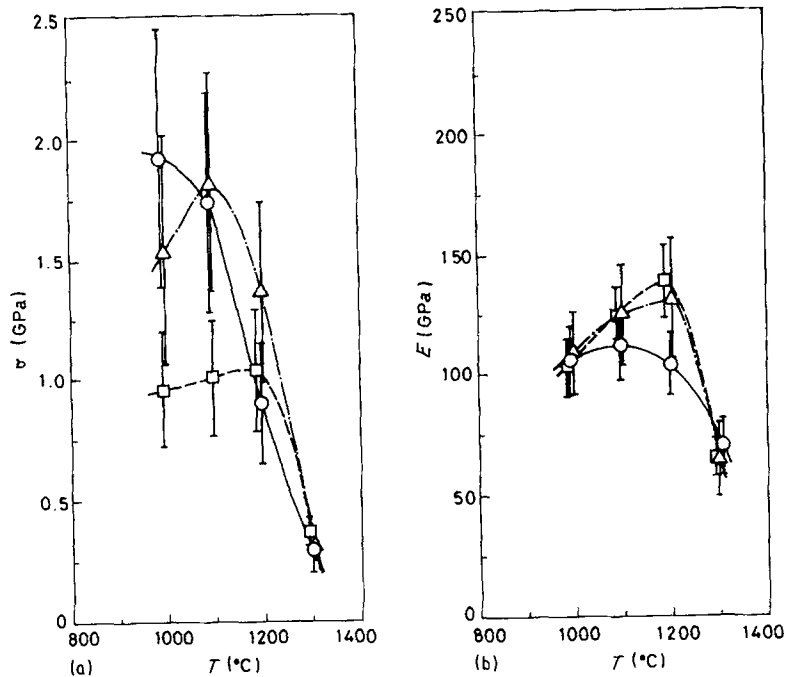*Figure 3* The relation between (a) tensile strength (σ) and (b) Young's modulus (E) and the heat-treatment temperature in the fibres obtained from (○) PC-Ti(0.07)$_{\text{III}}$ (T_c = 110°C), (△) PC-Ti(0.07)$_{\text{III}}$ (T_c = RT) and (□) PC-Ti(0.15)$_{\text{III}}$ (T_c = RT) in a vacuum.

1100 to 1200 °C heat-treatment temperature. In a previous paper [1], it was presumed that the reason for the decreasing mechanical properties of the Si-Ti-C-O fibre at high heat-treatment temperature was the formation and crystallization of β-SiC.

Fig. 4 shows infrared spectra of the fibres obtained from PC-Ti(0.15)$_{\text{III}}$ (T_c = RT). It can be seen that the Si-O-Si bond (1080 cm^{-1}) almost disappears at 1300 °C. In Fig. 5, X-ray diffraction patterns of the fibres obtained from PC-Ti(0.07)$_{\text{III}}$ (T_c = 110 °C) and PC-Ti(0.15)$_{\text{III}}$ (T_c = RT) are shown. In both the fibres obtained at 1300 °C, the peaks due to β-SiC and

Figure 4 Change in infrared spectrum with heat-treatment temperature in the fibre obtained from PC-Ti(0.15)$_{\text{III}}$ (T_c = RT) in a vacuum.

TiC are observed at 2θ ≃ 35.8, 41.8, 60.2, 72.0 and 75.9° [1]. However, the peaks are broad at a temperature of 1200 °C or below. Therefore, it can be seen that the structural change of the fibre is drastic in the temperature range 1200 to 1300 °C. Fig. 4 shows the drastic decrease of the Si-O bond in the fibre in this temperature range. Consequently, it is assumed that above 1200 °C, β-SiC and TiC crystallize, so that the mechanical properties of the fibre rapidly decrease.

The above crystallization is characterized by CO gas evolution which has been studied in detail for SiC fibre obtained from PC [3, 4]. In Fig. 6, the gas evolution curve of PC-Ti(0.15)$_{\text{III}}$ fibre (T_c = RT) in the pyrolysis process is shown. It can be seen that the thermal decomposition of the polysilane skeleton at 400 to 600 °C and of the side chains at 600 to 800 °C occur. Above 1250 °C, a considerable gas evolution is observed and, further, two sharp peaks at 1260 and 1290 °C overlap. These peaks correspond to that of cured PC fibre in the temperature range 1330 to 1350 °C. From these results, it is suggested that the activity of oxygen in SiC and Si-Ti-C-O fibres differs. The CO gas evolution occurs by reaction between oxygen and excess carbon, resulting in β-SiC formation and crystallization in the grain boundary and decrease of the fibre strength.

Titanium in the polymer forms a Ti-C bond in the initial stage of pyrolysis previously described. From Fig. 3, the higher the content of titanium in the fibre, the lower the tensile strength becomes, but the Young's modulus does not decrease. In addition, the influence of oxygen introduced by curing on the mechanical properties of the fibre is larger than that of oxygen in titanium alkoxide and, consequently, decrease in the tensile strength and Young's modulus of Si-Ti-C-O fibre from PC-Ti(0.07)$_{\text{III}}$ (T_c = 110 °C) occurs at lower heat-treatment temperatures as shown in Fig. 3.

The relation between the pyrolysis process of the polymer in an inert gas atmosphere and the structure will be reported in the near future.
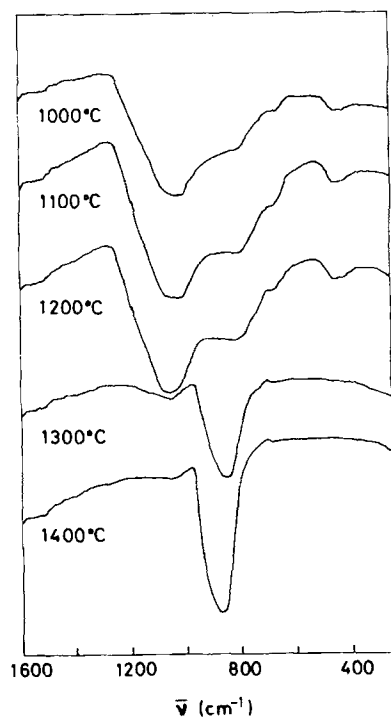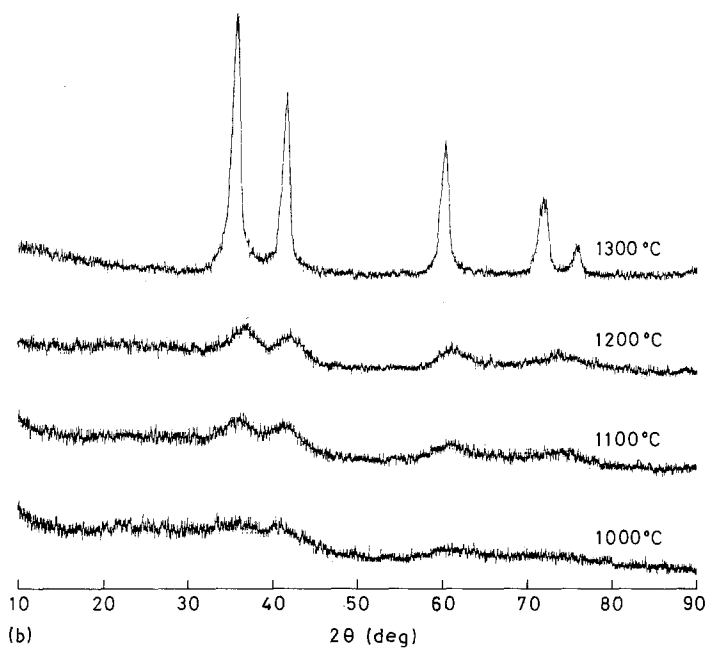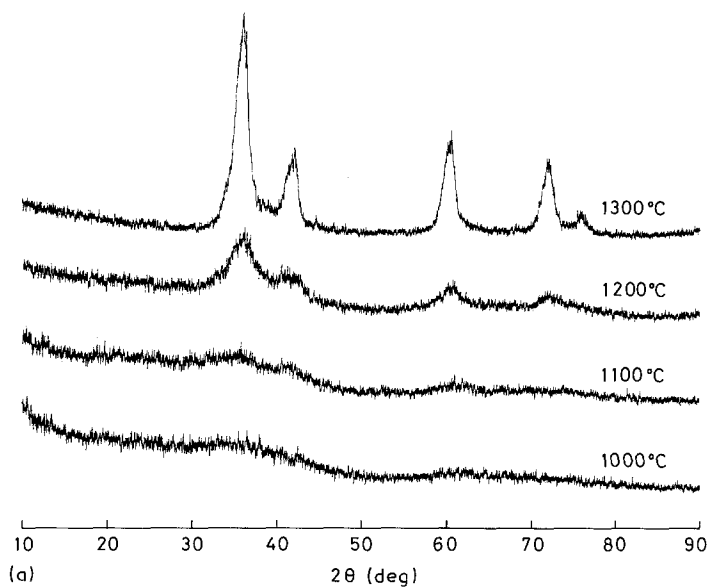
3.3. Si–Ti–O fibre

It is expected that a continuous Si–Ti–O fibre may be produced readily with PC containing Si–O–Ti bonds as the precursor.

The relation between the mechanical properties of Si–Ti–O fibre obtained from PC–Ti(0.15)$_{III}$ $(T_c = RT$ or $110\,°C)$ and the heat-treatment temperature in an oxygen gas flow is shown in Fig. 7. The fibre

obtained is colourless and transparent, and contains no carbon. The SiO_2–TiO_2 fibres so far reported were synthesized by the sol–gel method with metal alkoxides [5, 6] and from polytitanosiloxanes obtained by condensation between silicic acid and bis(2,4-pentanedionato)-titanium diisopropoxide [7]. The
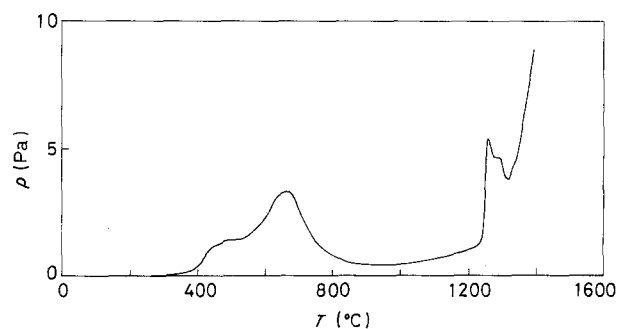

Figure 6 Gas evolution curve of PC–Ti(0.15)$_{III}$ fibre $(T_c = RT)$ in the pyrolysis process.

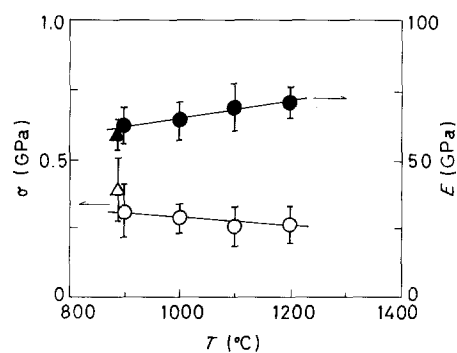Figure 7 The relation between tensile strength (σ) and Young's modulus (E) and heat-treatment temperature in the fibre obtained from PC–Ti(0.15)$_{III}$ $(T_c = (\bigcirc, \bullet) RT, (\triangle, \blacktriangle) 110\,°C)$ in an oxygen gas flow.
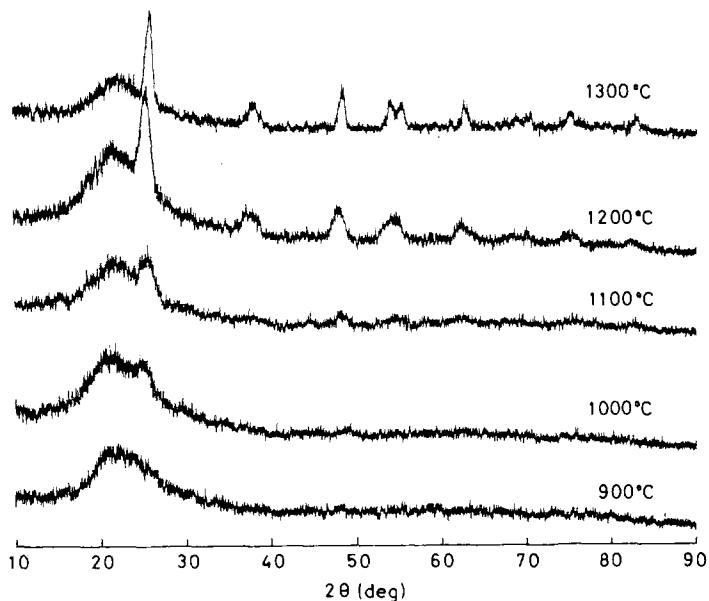
Figure 8 Change in X-ray diffraction pattern (CuK$_\alpha$) with heat-treatment temperature in the fibre obtained from PC-Ti(0.15)$_\text{III}$ (T_c = RT) in an oxygen gas flow.

mechanical properties of these fibres have not been reported. The tensile strength of Si–Ti–O fibre in this study is almost the same as that of a gel-derived SiO$_2$ fibre [8, 9]. Further, in Fig. 7, the tensile strength is retained and Young's modulus increases gradually up to 1200 °C heat-treatment temperature, while the tensile strength of gel-derived SiO$_2$ fibre decreases above 900 °C [8]. Thus, it is clear that the heat-resistivity of Si–Ti–O fibre is higher than that of gel-derived SiO$_2$ fibre. Above 1300 °C heat-treatment temperature, Si–Ti–O fibres obtained were stuck to each other, so that measuring the mechanical properties of the fibre was difficult.

In Fig. 8, X-ray diffraction patterns of Si–Ti–O fibre obtained from PC-Ti(0.15)$_\text{III}$ (T_c = RT) are shown. The diffraction lines assigned to anatase become distinct with increasing heat-treatment temperature. In TiO$_2$ fibre obtained by sol–gel method with TPT, anatase appeared on heat-treatment at 150 °C and was converted into rutile above 700 °C [10]. In TiO$_2$ obtained after fibre unidirectional freezing of the gel, the phenomenon is similar to that described above [11]. On the other hand, in SiO$_2$–TiO$_2$ gels obtained by condensation between silicic acid and titanium chelates, a gel containing not more than 50 mol % TiO$_2$ is amorphous even after heat-treatment at 1000 °C, and in that with more than 50 mol % TiO$_2$, anatase and rutile crystallize at lower temperature [12]. However, in the fibre heat treated at 1030 °C, anatase and rutile crystallized even at Ti/Si = 0.3 [7]. In Si–Ti–O fibre, crystallization of rutile is not observed in Fig. 8.

The infrared spectra of Si–Ti–O fibre obtained from PC-Ti(0.15)$_\text{III}$ (T_c = RT) are shown in Fig. 9. Peaks at 1080, 800 and 460 cm^{-1} are due to the Si–O–Si bond. A peak at 920 to 940 cm^{-1} is due to the Si–O–Ti bond. The peak intensity decreases with increasing heat-treatment temperature and, at the same time, the intensity of a new peak at 600 to 700 cm^{-1} increases. This new peak agreed with that of Ti–O stretching observed in TiO$_2$ powder. Consequently, the structure of Si–Ti–O fibre is amorphous at 900 °C, because titanium are isolated

from each other because of the Si–O–Ti bond. With increasing heat-treatment temperature, TiO$_2$ should separate out gradually; this is supported by the results of X-ray diffraction measurement in Fig. 8.

The pyrolysis process of the precursor in an oxygen gas flow has not been studied in detail. In comparison with the sol–gel method [12, 13], the infrared spectra of Si–Ti–O fibre during pyrolysis show smaller peaks due to residual water and the Si–OH group (3650 to 3200 cm^{-1} and 1620 cm^{-1}), because water was not

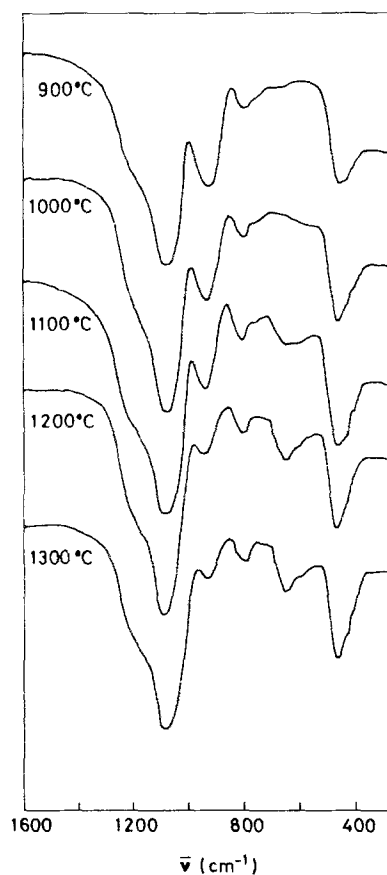*Figure 9* Change in infrared spectrum with heat-treatment temperature in the fibre obtained from PC-Ti(0.15)$_\text{III}$ (T_c = RT) in an oxygen gas flow.

used as a solvent and no Si-OH groups were present in the precursor. This means that evolution of water occurs in the pyrolysis process and a dense glass must be produced. However, the skeleton of the polymer is PC and, consequently, carbon atoms exist in the main chain and the side chain in the polymer. These carbon atoms are oxidized and are evolved from the fibre. The amounts of carbon evolved and oxygen introduced are very large, because the carbon content in PC is 36 to 40 wt % and the atomic ratio $C/Si \simeq 2$ [3]. Finally, it is estimated that exchange between carbon and oxygen occurs at the atomic ratio $C/O \simeq 1$.

The oxidation mechanism of PC has been discussed previously from the TG-DTA curve in air [4]. The curve shows that the oxidation mechanism is not a simple exchange between carbon and oxygen. At low temperature, Si-H bonds are mainly oxidized as are some of the methyl groups. Also, in PC, such as PC-B synthesized at low reaction temperature, the residual polysilane skeleton in the PC skeleton is oxidized directly into the siloxane skeleton [4]. Thus, by oxidation of the Si-H bond to Si-OH, and the polysilane skeleton to the siloxane skeleton, a considerable weight gain (10 to 15 wt % up to 200 °C in PC-B) occurs in the initial stage of oxidation. In the next stage, methyl groups are mainly oxidized to Si-OH which contribute very little to weight gain, and then dehydration between Si-OH groups becomes predominant, resulting in weight loss. Although it is not clear when oxidation of methylene and methane groups forming the PC skeleton occurs, it must be at higher temperature and siloxane bonds form directly without weight gain. Thus, the weight residue of PC after complete oxidation is about 100% [4].

It is assumed that the oxidation mechanism of PC-Ti(0.15)$_{III}$ is the same as that of PC-B. That is, 15% weight gain begins from about 100 °C and then weight loss occurs from about 400 °C. However, residual alkoxy groups in PC-Ti(0.15)$_{III}$ may further complicate the pyrolysis process.

The relation between the structural change in Si-Ti-O fibre, especially crystallization of anatase, and the mechanical properties will be studied in the near future.

3.4. Si-Ti-O-N fibre

The synthesis of Si-N-O fibre by heat-treating PC fibre in an ammonia gas flow has been reported [14-16]. Although the relation between the structure and mechanical properties of the fibre has not become sufficiently apparent, the appearance of the strength in the fibre is attributable to the amorphous structure, and the mechanical properties are correlated with oxygen content in the fibre [15].

By heat treating PC-Ti(0.15)$_{III}$ fibre in an ammonia gas flow, Si-Ti-O-N fibre was synthesized. Thus far, Si-Ti-O-N fibre has not been reported, but it has been reported that TiN fibre is synthesized by nitridation of TiO$_2$ gel fibre [17]. In this case, formation of TiN begins at 900 °C in ammonia gas flow and electrical conductivity appears. However, the mechanical properties of TiN fibre are not described.
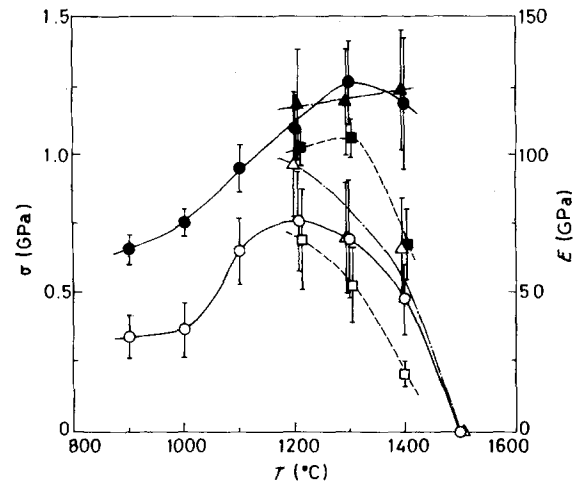

Figure 10 The relation between tensile strength (σ) and Young's modulus (E) and heat-treatment temperature in the fibres from PC-Ti(0.15)$_{III}$ in ammonia gas flow. ($\bigcirc$) σ, ($\bullet$) E, T_c = RT. ($\triangle$) σ, ($\blacktriangle$) E, T_c = 180 °C. ($\square$) σ, ($\blacksquare$) E, T_c = 250 °C.

Fig. 10 shows the relation between the mechanical properties of Si-Ti-O-N fibres obtained from PC-Ti(0.15)$_{III}$ cured at various T_c and heat-treatment temperatures. The tensile strength increases up to 1200 °C and then decreases. Young's modulus increases up to 1400 °C. Above 1200 °C the mechanical properties of Si-Ti-O-N fibre are higher than those of Si-Ti-C-O fibre as shown in Fig. 3. On the other hand, below 1000 °C, these properties are almost the same as those of Si-Ti-O fibre, as shown in Fig. 7. Studying these results, the relationship between the mechanical properties and the structure of the fibre may be clarified.

The carbon content in Si-Ti-O-N fibre obtained from PC-Ti(0.15)$_{III}$ (T_c = RT) at 1200 °C is 0.88 wt %. The colour of the fibre changed with increasing heat-treatment temperature, i.e. black → deep purple → brown.

In Fig. 11, infrared spectra of Si-Ti-O-N fibres obtained from PC-Ti(0.15)$_{III}$ (T_c = RT) are shown. Up to 1000 °C heat-treatment temperature, a peak at 1400 cm^{-1} is observable. This peak is attributable to Si-NH- [18] or Si-NH$_2$ [19] and, consequently, there should exist a large number of N-H bonds in the fibre. At 1100 °C, this peak disappears and, at the same time, the tensile strength increases as shown in Fig. 10. The absorbance at 700 to 1000 cm^{-1} increases up to 1300 °C which indicates an increase in the number of Si-N-Si bonds. Further, a peak exists at about 940 cm^{-1}, in agreement with that of Si-O-Ti bonds in Fig. 9. Above 1300 °C, the absorbance at 700 to 1000 cm^{-1} and a peak intensity at about 940 cm^{-1} decrease. Consequently, the decrease in tensile strength of the fibre above 1300 °C in Fig. 10 may be correlated with the decrease in the number of Si-N-Si and Si-O-Ti bonds.

Fig. 12 shows X-ray diffraction patterns of these fibres. In the fibre obtained at 1500 °C, the sharp diffraction lines due to TiN are observable at $2\theta \simeq 36.9$, 42.8, 62.1, 74.4 and 78.3° [17]. The broad peak at $2\theta \simeq 22°$ is the same as that in silicon oxynitride [14-16], and is shifted to $2\theta \simeq 24°$ below 1000 °C. As the heat-treatment temperature decreases,
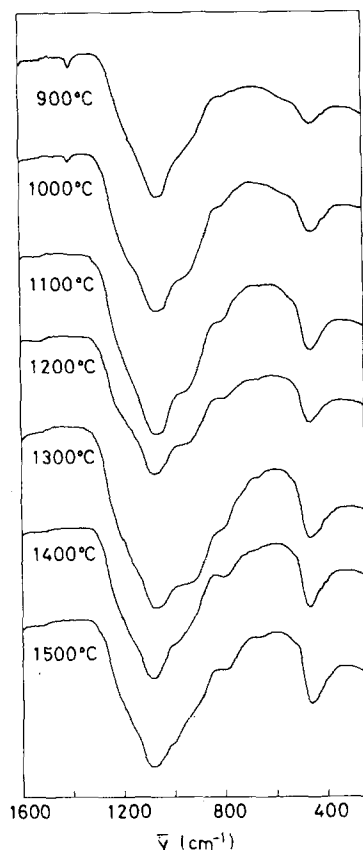
Figure 11 Change in the infrared spectrum with heat-treatment temperature in the fibre obtained from PC–Ti(0.15)$_{III}$ (T_c = RT) in ammonia gas flow.

the peaks due to TiN become broad, so that the structure is amorphous.

As T_c increased, the peak at 1080 cm^{-1} due to the Si–O–Si bond in the infrared spectra and the peak at $2\theta \simeq 22°$ in the X-ray diffraction pattern became comparatively strong. This tendency was almost independent of heat-treatment temperature and was evident at T_c > 180 °C. The mechanical properties of the fibres obtained at 1200 °C increased gradually up to

T_c = 180 °C and then decreased. Above 180 °C, oxidation of the methyl group predominantly occurs in the curing process as described previously. However, the relation between the mechanical properties and oxidation of the methyl group is not clear.

From the above results, the structure of Si–Ti–O–N fibre is composed of Si–O–Si, Si–O–Ti, Si–N and Ti–N bonds in an amorphous state at low heat-treatment temperature, and then, as the temperature increases, TiN crystallizes with decrease of the tensile strength. The abrupt crystallization of TiN above 1400 °C is shown by scanning electron micrographs of Si–Ti–O–N fibre obtained from PC–Ti(0.15)$_{III}$ (T_c = 180 °C) in Fig. 13. In the cross-sections of the fibres, no pores are seen at 1200 and 1300 °C, but some are present at 1400 °C. At 1500 °C, however, the fibres are significantly deformed which may show thermal decomposition in the fibre. It is assumed that Ti–N and Si–O–Si bonds were formed by decomposition of Si–N–Si and Si–O–Ti bonds (Figs 11 and 12). Nitridation of TiO$_2$ gel fibre occurs at 900 °C and TiN with high crystallinity is formed [17], whereas the crystallinity of TiN formed by nitridation of PC–Ti(0.15)$_{III}$ fibre is low. Consequently, this supports the uniform distribution of titanium atoms in Si–Ti–O–N fibre and the holding of the Si–O–Ti bond to high temperature.

The measurement of electrical conductivity of the Si–Ti–O–N fibre may be effective in studying the formation process of TiN.

4. Conclusion

It was found that Si–Ti–C–O, Si–Ti–O and Si–Ti–O–N fibres are synthesized from PC containing titanium alkoxide as pendant groups. The polymer is thus useful for ceramic powders and bodies. The structure of the fibres is amorphous at low temperature. However, β-SiC and TiC at 1300 °C in Si–Ti–C–O fibre, anatase at 1200 °C in Si–Ti–O fibre, and TiN at
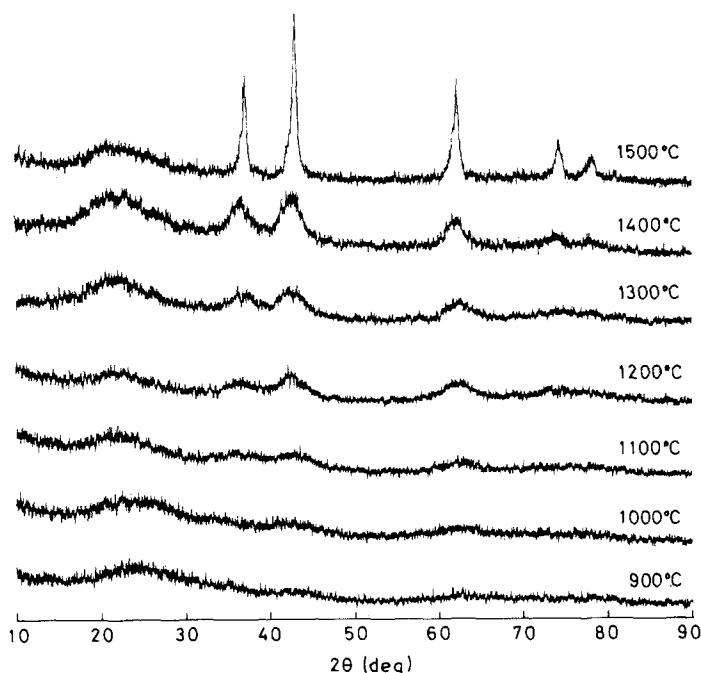

Figure 12 Change in X-ray diffraction pattern (CuKα) with heat-treatment temperature in the fibre obtained from PC–Ti(0.15)$_{III}$ (T_c = RT) in ammonia gas flow.
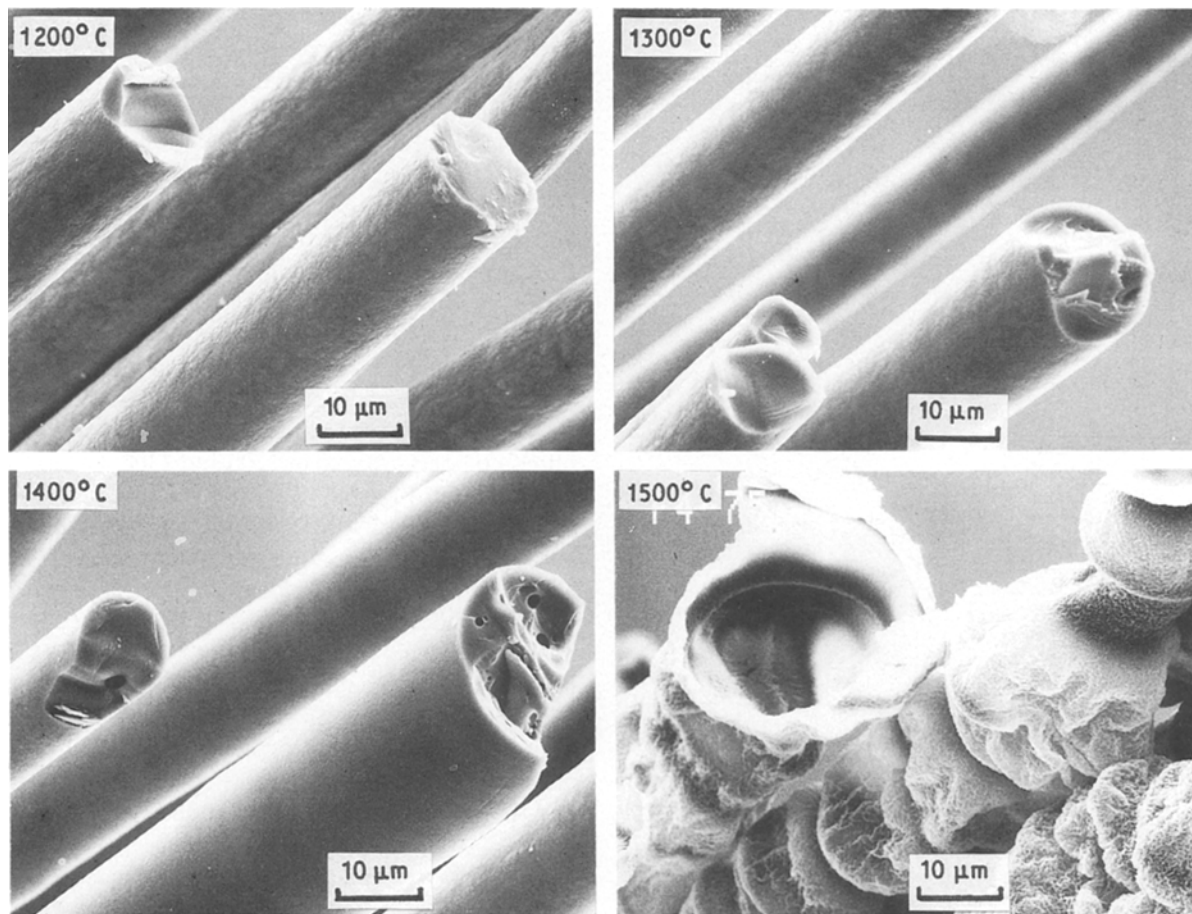
Figure 13 Scanning electron micrographs of Si–Ti–O–N fibres obtained at various heat-treatment temperatures in ammonia gas flow from PC–Ti(0.15)$_{III}$ (T_c = 180 °C).

1500 °C in Si–Ti–O–N fibre crystallize. A characteristic of ceramics obtained from PC containing Si–O–Ti bonds is crystallization of titanium compounds. By controlling the crystallization, these fibres should have new functions.

References

1. Y.-C. SONG, Y. HASEGAWA, S.-J. YANG and M. SATO, *J. Mater. Sci.* **23** (1988) 1911.
2. H. ICHIKAWA, F. MACHINO, S. MITSUNA, T. ISHIKAWA, K. OKAMURA and Y. HASEGAWA, *ibid.* **21** (1986) 4352.
3. Y. HASEGAWA and K. OKAMURA, *ibid.* **18** (1983) 3633.
4. Y. HASEGAWA, *ibid.* **24** (1989) 1177.
5. K. KAMIYA, S. SAKKA and N. TASHIRO, *Yogyo-Kyokai-Shi* **84** (1976) 614.
6. K. KAMIYA, S. SAKKA and S. ITO, *ibid.* **85** (1977) 599.
7. Y. ABE, T. GUNJI, M. HIKITA, Y. NAGAO and T. MISONO, *ibid.* **94** (1986) 1243.
8. S. SAKKA, *Hyomen* **19** (1981) 430.
9. W. C. LaCOURSE, "Better Ceramics Through Chemistry", edited by C. J. Brinker, D. E. Clark and D. R. Ulrich (North-Holland, Amsterdam, 1984) p. 53.
10. K. KAMIYA, K. TANIMOTO and T. YOKO, *J. Mater. Sci. Lett.* **5** (1986) 402.
11. T. MAKI, T. KOKUBO and S. SAKKA, *Bull. Inst. Chem. Res. Kyoto Univ.* **64** (1986) 292.
12. Y. ABE, N. SUGIMOTO, Y. NAGAO and T. MISONO, *J. Non-Cryst. Solids* **104** (1988) 292.
13. S. SAKKA and K. KAMIYA, *ibid.* **42** (1980) 403.
14. K. OKAMURA, M. SATO, Y. HASEGAWA and T. AMANO, *Chem. Lett.* (1984) 2059.
15. K. OKAMURA, M. SATO and Y. HASEGAWA, *Ceram. Int.* **13** (1987) 55.
16. M. SATO, Y. HASEGAWA and K. OKAMURA, *J. Ceram. Soc. Jpn Inter. Edn.* **95** (1987) 937.
17. K. KAMIYA, T. YOKO and M. BESSHO, *J. Mater. Sci.* **22** (1987) 937.
18. A. KATO, Y. ONO, S. KAWAZOE and I. MOCHIDA, *Yogyo-Kyokai-Shi* **80** (1972) 114.
19. R. C. G. SWANN, R. R. MEHTA and T. P. CAUGE, *J. Electrochem. Soc.* **114** (1967) 713.